Characteristics of variably saturated granular bentonite after long-term storage at near-field relevant temperatures

M. VALTER* AND M. PLÖTZE

ClayLab, Institute for Geotechnical Engineering, ETH Zürich, Schafmattstrasse 6, 8093 Zürich, Switzerland

ABSTRACT: Bentonite is a potential material for use in the engineered barrier of radioactive waste repositories because of its low hydraulic permeability, self-sealing capability and retention capacity. It is expected that bentonite would react at the elevated temperatures accompanying the radioactive decay in the nuclear waste. The presented study was started in order to improve understanding of the coupled influence of temperature and (pore) water on the physicochemical and mineralogical properties of bentonite during thermal treatment under near-field relevant conditions. Granular Na-bentonite MX-80 was differently saturated ($S_r = 1-0.05$) and stored at different temperatures ($50-150$ºC) in a closed system. Upon dismantling after different periods of time (3 to 18 months), mineralogical characteristics, cation exchange capacity and content of leachable cations, as well as physicochemical properties such as surface area and water adsorption were investigated.

The results showed a high mineralogical stability. A slight conversion from the sodium to an earth alkali form of the bentonite was observed. However, considerable changes in the physicochemical properties of the bentonite were observed, particularly by treatment above the critical temperature of 120ºC. The cation exchange capacity decreased during heating at 150ºC by approximately. 10%. The specific surface area dropped by more than 50%. The water uptake capacity under free swelling conditions showed a slight tendency to lower values especially for samples heated for more than 12 months. The water vapour adsorption ability in contrast drops by 25% already within three months at $T = 120$ºC. These changes are mostly related to the variations in the interlayer cation composition and to smectite aggregation processes. The observed alterations are rather subtle. However, temperatures $\geqslant 120$ºC had a remarkable negative influence on different properties of MX-80.

KEYWORDS: radioactive waste repository, thermal treatment, Na-bentonite, bentonite alteration.

In several countries, a deep geological repository is foreseen as the most suitable solution for the issue of radioactive waste disposal (Russell & Facella, 2006). Such an underground facility should isolate radioactive waste from the biosphere and ensure the dissipation of the heat of decay (Kahr & Müller Vonmoos, 1982). Currently designed repositories for radioactive waste are multibarrier systems composed of the natural barrier (host rock) and a combination of several engineered barriers (Nagra, 2002). An important part of the engineered barrier system is the bentonite backfill. The use of bentonite as the engineered barrier is of crucial importance because of its low hydraulic permeability, self-sealing capability and retention capacity (Pusch, 2001). Bentonite is a natural material, predominantly consisting of smectite, and represents a product of the early diagenetic alteration of vitric fallout ash in subaqueous, mainly marine environments (Chamley, 1989). Bentonite shows a great stability against weathering (Laine & Karttunen, 2010). Nevertheless, its properties can alter under harsh conditions such

* E-mail: martin.valter@igt.baug.ethz.ch

as elevated temperature and pressure or wetting-drying cycles (Galán, 2006; Pusch, 2006). The exposure of bentonite to hot steam leads to a decrease in swelling capability and to an increase in hydraulic conductivity, all of which are also mirrored in the bentonite microstructure (Couture, 1985; Pusch, 2000). It is expected that bentonite would react at the elevated temperatures accompanying the radioactive decay in the nuclear waste (Sato *et al.*, 1998). Temperatures below 50ºC in the repository bentonite buffer and its full saturation are expected within 100−200 years (Senger & Ewing, 2008). The swelling behaviour and geochemical reactions of bentonite have been studied by saturation with pore water solutions with different chemical composition and ionic strength under confined conditions at elevated temperatures in short-term laboratory experiments (Montes-H & Geraud, 2004; Herbert *et al.*, 2008; Kaufhold & Dohrmann, 2009, 2010, 2011; Gómez-Espina & Villar, 2010; Perdrial & Warr, 2011; Kasbohm *et al.*, 2012). Only minor alteration of the bentonite was reported. The described initial transformation of smectite to interstratified illite-smectite, and the decrease in layer charge are rather insignificant. Significant chemical changes are related to cation exchange processes only. The sorption ability of MX-80 remained unchanged up to 250ºC of heating for 24 h.

Several *in situ* experiments have been started in order to investigate the behaviour of bentonite under elevated temperature in the potential host rock in order to study the far-to-near-field conditions in detail. Some of these projects are the FEBEX in Grimsel (enresa, 2000) and the Heater Experiment in Mont Terri (Göbel *et al.*, 2006) both in Switzerland as well as the Alternative Buffer Materials project (ABM; Svensson *et al.*, 2011), and the Long Term Test of Buffer Material project (LOT; Olsson & Karnland, 2011), both situated in the Äspö Hard Rock Laboratory, Sweden. Generally, these experiments demonstrated a high chemical and mineralogical stability of the bentonite during thermal treatment. However, not all experiments showed the same reactions. The investigation of the thermo-hydro-mechanical (THM) properties of the bentonite after five years treatment at repository conditions in the FEBEX experiment revealed unchanged retention and swelling capacity (Villar & Lloret, 2007). The analysis of the treated bentonite from the HEATER experiment discovered slight alterations related to

cementing processes (by precipitation of amorphous Si/Al compounds). The specific surface area (SSA) decreased by about 20%. Besides the interlayer cation exchange an insignificant decrease of the mean layer charge (MLC) was detected (Plötze *et al.*, 2007). In the ABM project, besides slight tendencies of cation exchange, an increase in the cation exchange capacity (CEC) of the bentonite was measured in the direction of the heating source (Nagra, 2011; Svensson *et al.*, 2011). However, the differences appear to border the line of analytical error. As in the HEATER experiment, a significant decrease of the SSA of the MX-80 bentonite was measured as well. Additionally, in the LOT project, carbonate dissolution and gypsum dehydration in MX-80 according to the temperature gradient were observed. Close to the heater in the A2 parcel test, calcite was dissolved and gypsum dehydrated within the almost six-years of heating whereas gypsum precipitated in the colder and more humid part near the host rock (Olsson & Karnland, 2011).

The present study was started in order to improve the understanding of the coupled influence of temperature and (pore) water on the physicochemical and mineralogical as well as on the hydraulic and mechanical properties of bentonite during thermal treatment. The temperature and hydration state of the bentonite were adapted to the expected conditions in the near-field of a planned repository for radioactive waste (Fig. 1). In the experiment the
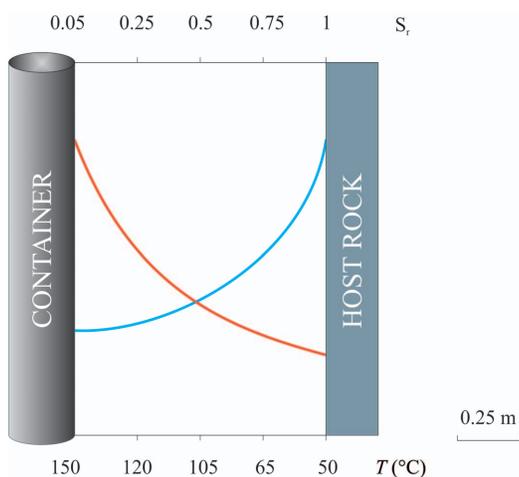
FIG. 1. Evolution of the saturation degree (blue curve) and temperature (orange curve) in the engineered barrier between the container and host rock (adapted from Senger & Ewing, 2008).

Na-bentonite MX-80 was used, which is one of the possible buffer materials. The bentonite was saturated with artificial pore water of the same chemical composition as the pore water of the Opalinus clay – a potential host rock for the radioactive waste repository in Switzerland. The thermal treatment was carried out under laboratory conditions in a small-scale closed system, providing full control of physical and chemical factors (mass and bulk density of the bentonite, content and chemical composition of the pore water, and temperature). The time scale of the experiment with more than three years of treatment will be in the same range as most of the *in-situ* long-term experiments.

The chosen set-up allows observation in short time steps of the initial changes in the important bentonite properties under near-field relevant conditions comparable with large-scale *in-situ* experiments but in a closed system under controlled environmental conditions.

MATERIALS AND DESCRIPTION OF THE EXPERIMENT

Bentonite

The Na-bentonite MX-80 (Wyoming, AMCOL International Corp.) was used in this experiment. The mineralogical composition of the bentonite is characterised by a high content of smectite and about 10 wt.% of mica-like minerals and tectosilicates each. In traces, cristobalite, calcite and gypsum were found but also pyrite (Table 1). The bentonite is a granular material from the ESDRED experiment (Engineering Studies and Demonstration of Repository Design), where different granulometric distributions were tested in emplacement studies (Plötze & Weber, 2007). The chosen granular mixture ESDRED "E" (uniformity index C_U = 13.22, curvature index C_C = 1.65, d_{50} = 1.61 mm, dry bulk density of bentonite granules ρ_d = 1.962 g/cm^3) achieved the highest dry emplacement density (ρ_d = 1.513 g/cm^3). Various portions of bentonite (26−46 g) were filled with a dry bulk density of ρ_d = 1.5 g/cm^3 in tight containers (Fig. 2). The containers consisted of an ematal-coated aluminium shell with an inner PTFE casing. The PTFE casing prevented contact of the bentonite material with the aluminium shell to avoid the formation of corrosion products in order to exclude an uncontrolled chemical influence. The containers

had an inner diameter of 40 mm and an inner height of 25 mm.

Artificial pore water

The bentonite was saturated with artificial pore water (APW) at five saturation degrees (S_r): 0.05, 0.25, 0.5, 0.75 and 1 (compare Fig. 1) corresponding to ratios of solution to dry clay weight of 0.02, 0.08, 0.19, 0.33 and 0.53, respectively. The chemical composition of the APW (pH 7.9, alkalinity 0.55, ionic strength 0.23, Na-Ca-Mg-K type, main cation Na) corresponded to the pore water of the Opalinus Clay formation in the Brown Dogger facies (Mäder, 2009). The precise chemical composition of the APW (Table 2) was calculated using Phreeqc (version 2.15.07) software and NAGRA-PSI database Version 01/01.

Thermal treatment

The variably saturated bentonite were stored in the tight containers at temperatures (50, 65, 105, 120, and 150ºC) according to the expected temperature conditions at the different distances between the canister with the radioactive waste and the host rock (Fig. 1; Senger & Ewing, 2008). Accordingly, bentonite with S_r = 1 was stored at 50ºC (vicinity of the host rock) and the S_r = 0.05 sample at 150ºC (vicinity of the canister). One container was prepared for each temperature level and heating time. The heating time intervals were 3,

FIG. 2. Containers (ematal aluminium with inner PTFE casing) encapsulating granular MX-80 (dry bulk density 1.5 g/cm^3) during thermal treatment. The inhomogeneous water distribution (saturation degree 75%) is visible. The dark granules had a higher water content.

TABLE 1. Mineral composition of the bentonite MX-80 before and after the thermal treatment.

| | Pristine | | 3 months of thermal treatment | | | | | | | | | | 6 months | | | | | | | | |
| | | | 50°C | | 65°C | | 105°C | | 120°C | | 150°C | | 50°C | | 65°C | | 105°C | | 120°C | | 150°C | |
	Wt.%	±*	Wt.%	±	Wt.%	±	Wt.%	±	Wt.%	±	Wt.%	±	Wt.%	±	Wt.%	±	Wt.%	±	Wt.%	±	Wt.%	±
Bassanite	n.d.	n.d.	n.d.	n.d.	n.d.	n.d.	0.6	0.2	0.8	0.2	0.9	0.2	n.d.	n.d.	n.d.	n.d.	1.0	0.3	1.0	0.2	1.0	0.2
Calcite	1.0	0.1	1.2	0.2	1.0	0.2	0.8	0.2	0.7	0.1	0.5	0.2	1.0	0.2	0.8	0.2	0.3	0.2	0.7	0.2	0.5	0.1
Cristobalite	2.2	0.2	1.8	0.3	2.0	0.3	2.2	0.2	2.1	0.2	2.0	0.2	1.9	0.2	2.0	0.2	1.9	0.2	1.8	0.2	1.9	0.2
Gypsum	0.8	0.3	1.8	0.3	1.8	0.3	n.d.	n.d.	n.d.	n.d.	n.d.	n.d.	0.8	0.2	0.9	0.3	n.d.	n.d.	n.d.	n.d.	n.d.	n.d.
Mica/S.c.l.	12.4	1.5	9.4	1.2	11.8	1.2	12.5	1.6	11.6	0.9	9.1	1.0	13.3	0.8	13.9	0.8	8.2	1.1	12.4	0.8	12.5	0.9
Feldspat	4.5	0.7	7.3	1.1	6.5	0.9	5.1	0.7	4.4	0.7	5.0	0.9	5.0	0.9	5.5	0.9	5.8	0.8	6.9	0.9	4.9	0.8
Pyrite	0.5	0.1	0.3	0.1	0.4	0.1	0.3	0.1	0.4	0.1	0.4	0.1	0.2	0.1	0.3	0.1	0.2	0.1	0.4	0.1	0.3	0.1
Quartz	6.0	0.2	5.9	0.3	5.8	0.3	5.8	0.2	6.1	0.2	5.9	0.2	5.4	0.2	5.4	0.2	5.7	0.3	5.1	0.2	5.2	0.2
Smectite	72.7	1.2	72.3	1.2	70.8	1.3	72.8	1.2	73.9	1.1	76.3	1.0	72.3	1.0	71.2	1.0	76.8	1.2	71.8	0.9	73.7	1.1

| | 12 months | | | | | | | | | | 18 months | | | | | | | | | |
| | 50°C | | 65°C | | 105°C | | 120°C | | 150°C | | 50°C | | 65°C | | 105°C | | 120°C | | 150°C | |
	Wt.%	±	Wt.%	±	Wt.%	±	Wt.%	±	Wt.%	±	Wt.%	±	Wt.%	±	Wt.%	±	Wt.%	±	Wt.%	±
Bassanite	n.d.	n.d.	n.d.	n.d.	0.5	0.2	0.8	0.2	1.4	0.2	n.d.	n.d.	n.d.	n.d.	0.7	0.2	0.8	0.2	0.9	0.2
Calcite	0.9	0.2	0.9	0.2	0.4	0.1	0.7	0.1	0.4	0.2	0.7	0.2	0.7	0.1	0.4	0.3	0.6	0.2	0.6	0.2
Cristobalite	2.0	0.1	2.3	0.2	1.9	0.2	1.8	0.2	2.0	0.2	1.9	0.2	2.0	0.2	1.9	0.2	2.0	0.2	1.9	0.2
Gypsum	1.0	0.3	1.9	0.5	n.d.	n.d.	n.d.	n.d.	n.d.	n.d.	1.7	0.3	2.2	0.4	n.d.	n.d.	n.d.	n.d.	n.d.	n.d.
Mica/S.c.l.	15.1	1.1	10.5	1.3	11.7	0.9	12.3	1.0	12.3	1.4	14.1	1.4	14.1	1.4	12.8	1.5	14.5	1.7	13.2	1.5
Feldspat	5.4	1.0	6.6	1.0	5.5	0.7	4.1	0.9	6.5	0.8	5.7	0.9	7.5	0.9	6.3	0.9	7.2	1.0	6.6	0.9
Pyrite	0.2	0.1	0.0	0.1	0.2	0.1	0.3	0.1	0.2	0.1	0.2	0.1	0.1	0.1	0.2	0.1	0.3	0.1	0.3	0.1
Quartz	4.7	0.2	6.1	0.3	5.3	0.2	4.9	0.2	5.6	0.3	5.5	0.2	5.7	0.3	5.4	0.2	5.5	0.3	5.5	0.2
Smectite	70.7	1.2	71.7	1.4	74.4	1.1	74.9	1.2	71.7	1.5	70.3	1.1	67.7	1.1	72.3	1.1	69.0	1.4	71.1	1.2

n.d. – not detected; *3σ absolute error

TABLE 2. Artificial pore water (APW) characteristics corresponding to the chemical composition of the pore water in Opalinus clay.

Temperature (ºC)	25			
pH	7.861			
	(mmol/kg)	(g/L)	Alkalinity	0.5494
Na (total)	163.8	3.766	P (CO$_2$)	1E-3.5
K (total)	2.551	0.1	Ionic strength	0.2264
Ca (total)	11.91	0.477	SI (calcite)	0
Mg (total)	9.166	0.223	SI (dolomite, ord.)	0
Cl (total)	160	5.672	SI (gypsum)	−0.31
S^{6+} (total)	24	0.77		
C^{4+} (total)	0.5431	0.007		

6, 12 and 18 months. The material was then taken out of the container, dried overnight at 50ºC, crushed in an agate mortar and homogenized for further analysis.

ANALYTICAL METHODS

Mineralogical characterization

X-ray diffraction analysis. The samples were characterized by X-ray powder diffraction using a Bruker AXS D8 Advance diffractometer (source Co-$K\alpha$ radiation $\lambda = 1.790$ Å) equipped with primary and secondary soller and automatic theta compensating divergence and antiscatter slits. Data were collected from 2–80º2θ (2–40º2θ for textured specimens) with a step size of 0.02º2θ and a counting time of 4 s/step. The mineral composition of the samples was determined on randomly oriented powder and textured smear specimens. The samples were micronized in ethanol to <20 μm using a McCrone micronizing mill equipped with agate grinding elements. After drying, the samples were front-loaded into the sample holders by taping a razor blade onto the sample within the sample holder in order to, both, maximize the random orientation of the minerals and to achieve a flat surface of the sample (Zhang *et al.*, 2003). The textured specimens were prepared to easier identify the clay minerals. The basal reflections of the oriented clay minerals are enhanced through this technique (Brindley & Brown, 1980). An amount of each sample was mixed with deionised water. The paste was smeared onto the flat glass, dried in the laboratory atmosphere and analysed. The textured specimens were then saturated with ethylene glycol (EG) to examine smectite swelling (MacEwan & Wilson, 1980). The (00l) diffraction peaks can be observed as a rational series of *d* values for a discrete clay mineral. The coefficient of variation (CV) for the (00l) diffractions of samples saturated with propane−1,3−diol (instead of EG) were determined in order to detect the possible formation of interstratified irregular illite/smectite with a CV ⩾ 0.75 (Moore & Reynolds, 1997). The XRD was also used for the determination of the mean layer charge (MLC). The samples were intercalated with dodecyl ammonium (chain length nC = 12) and washed with ethanol (Lagaly, 1994). A few milligrams of talc were added to the intercalated samples as a line positioning standard for the XRD pattern. The prepared suspension was then dropped onto a glass slide, dried in vacuum at 40ºC and immediately measured. The MLC was calculated as MLC = [d_{001} − 5.52]/32.98 (Olis *et al.*, 1990). The determination of the basal spacing, as well as the qualitative phase analyses were carried out by processing the diffraction pattern in the DIFFRACplus EVA software (Bruker AXS). The quantitative composition was calculated by Rietveld analysis using the BGMN®/AutoQuan software (Bergmann & Kleeberg, 1998).

FTIR spectroscopy. The Fourier Transform Infrared Spectroscopy (FTIR) was used as an additional method for the mineral composition analysis. Particularly, the presence of amorphous silica and the ion allocation in the octahedral position in smectite were investigated (Madejová *et al.*, 2011). The IR spectra were measured in the middle-infrared region (4000−380 cm^{-1}) with a Perkin Elmer FTIR 2000 device. The measurements were carried out in transmission mode using KBr

pellets with two different weights (0.5 mg and 3 mg in 200 mg of KBr) for each sample.

Thermal analysis. Thermogravimetric and mass spectrometric analysis (TG-MS) was used as additional diagnostic tool particularly for the investigation of the dehydration and dehydroxylation characteristics of the smectite, the latter particularly for the analysis of the cis-/trans-vacancy character of its octahedral sheet (Emmerich, 2011). The measurements were carried out with a thermobalance Mettler-Toledo TGA/SDTA851[e]. With the coupled mass spectrometer Balzers ThermoStar GSD 300T the evolved water, CO_2 and SO_2 were investigated as a part of the mineral composition analysis. 110 mg of each sample was thermally analysed in a platinum crucible over the range 25−1000ºC (heating rate 10ºC/min) in a dry and CO_2-free airflow atmosphere (50 mL/min).

Cation exchange capacity, leachable cations and pore water chemistry. The CEC of the samples was determined using the complexes of copper (II) with triethylenetetramine (Meier & Kahr, 1999). The CEC should be comparable with the amount of exchangeable cations that entered the exchanging solution. However, this amount of exchangeable cations is not only represented by the interlayer cations, but also includes the dissolved cations in the pore water (including the added APW) and additionally, the cations from the soluble minerals dissolved during the exchange procedure. Therefore, the term "amount of exchangeable cations" was replaced here with the "amount of leachable cations" (ALC). The ALC was determined by the analysis of cation concentrations (Na^+, K^+, Mg^{2+}, Ca^{2+}) in the exchanging solutions after CEC measurement using atomic absorption spectrometry (AAS; device Perkin Elmer AAnalyst400). The chemistry of the pore water itself was determined by three times washing 2 g of each sample (in replicates) in 15 mL methanol. The suspension was centrifuged and the supernatant decanted and analysed by AAS.

Physical and physicochemical properties

Specific surface area determination by gas adsorption. The SSA represents ideally the external surfaces of crystals excluding the interlayers of sheet silicates but is for bentonites also influenced by the microporosity (Kaufhold *et al.*, 2010b). The SSA of the samples (300−700 mg) was determined

by N_2 adsorption using an 11-point BET method (Brunauer *et al.*, 1938). The adsorption isotherm measurements were carried out with a Quantachrome Autosorb-1MP surface area analyser (N_2 relative pressure p/p_0 0.05−0.3).

Water vapour adsorption and water uptake under free swelling conditions. The ability of MX-80 to adsorb water vapour was determined in an atmosphere with a relative humidity (RH) of 75% (Keeling *et al.*, 1980), which was achieved in a closed desiccator above an oversaturated NaCl solution (Madsen & Kahr, 1992). The sample weight was checked until constant weight (after ~6−9 weeks). The water content of such a treated sample (dried at 105ºC until weight constancy) (DIN ISO 11465, 1996) represents the level of the water vapour adsorption ability (WVAA).

The uptake capacity for liquid water under free swelling conditions was determined with the Enslin-Neff technique (DIN 18132, 1995; Kaufhold *et al.*, 2010a). About 85 mg of each sample (particles <400 μm) was used for the analysis. The water-uptake capacity (WUC) was related to the initial dry weight of the bentonite, taking into account the separately determined initial water content. The influence of evaporation during the measurements was eliminated by subtracting the evaporation determined in a separate Enslin-Neff apparatus filled with milled quartz.

To investigate the possible influence of heating on the gas adsorption behaviour of the bentonite (smectite aggregation/cementation, Couture effect), the SSA and WVAA were measured on selected samples again after remoulding. It is expected that the shearing in excess of water will break up the aggregates. The remoulding was carried out by mixing a certain amount of the differently treated bentonite (approximately 2 g) with deionized water and mechanically shearing with a pestle to form a homogeneous paste without lumps. After air-drying at ambient conditions, the samples were crushed in an agate mortar and homogenized.

RESULTS

Mineralogical characterization

The mineral composition of the pristine and the thermally treated MX-80 is shown in Table 1. The bentonite underwent some slight changes in mineral composition during the thermal treatment. The gypsum content in the pristine material was

1.0±0.3 wt.% and did not change in the samples stored at temperatures below 105ºC. No gypsum was found in the samples stored at $T > 65$ºC due to its dehydration and simultaneous bassanite formation. The calcite content in the pristine and treated MX-80 varies between 0.5−1.0±0.3 wt.%. However, the ambiguous tendency of its decrease with temperature borders the line of the analytical error. No amorphous silica was detected by FT-IR analysis (Fig. 3a,b). The smectite content seems to be slightly reduced over time regardless of treatment temperature. The sum of mica and mica-type layers/collapsed smectite layers showed a weak opposite tendency (Fig. 4a,b). However, this

increase is in the range of measurement error as well as additionally influenced by the heterogeneity of the pristine MX-80 and therefore rather ambiguous. The coefficient of variation (CV) in the basal spacing was determined for two specific samples to prove this increase of the content of mica-type layers as a tendency of illitization, which would be probably connected with the formation of interstratified illite/smectite (I/S). The CV of the pristine material was 0.2. For the sample with the highest content of mica and mica-type layers/collapsed smectite, which was the sample heated at 120ºC for 12 months, a CV of 0.38 was calculated. This insignificant increase does not
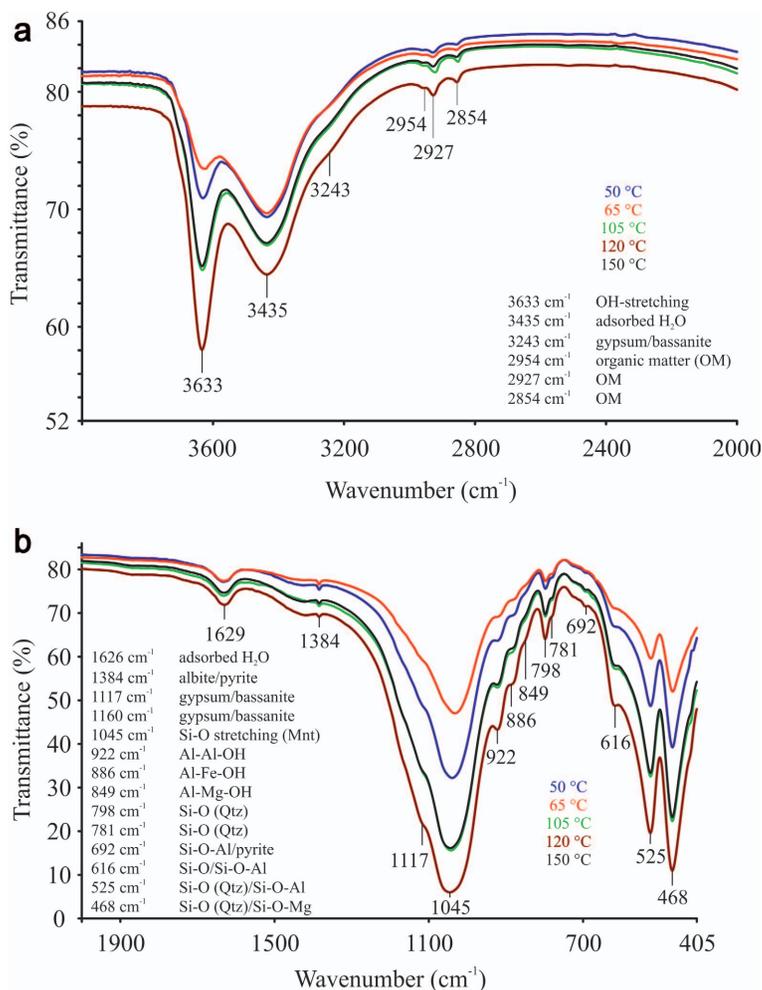
FIG. 3. The IR transmission spectra of MX-80 stored for 12 months at 50−150ºC. No band of amorphous silica at approximately 1090 cm^{-1} was observed.

indicate illitization. The slight increase of the MLC from 0.27−0.28 for samples heated up to three months to values of 0.29−0.30 for longer heated samples seemed to show the transformation of the smectite into a higher-charged form (Table 3). However, considering the measurement error of 6−13% (Lagaly & Weiss, 1969) all measured changes of MLC lay within the measurement error. The thermal analyses revealed for bentonites with higher saturation degree $S_r = 1$ and 0.75 stored at 50 and 65ºC, respectively, a shoulder at approximately 140ºC in their dehydration curves (Fig. 5a). The dehydroxylation curves showed an unchanged *cis-/trans*-vacant character of the smectite in all samples (Fig. 5b). No change in the basal distances (17.0 Å) of the smectite saturated with EG was observed (Fig. 6). The small shift of the basal (00l) spacing of smectite from pristine 12.3 Å towards 12.5 Å would indicate a partial replacement of interlayer Na^+ by bivalent cations. However, these measurements were not carried out under controlled relative humidity and are therefore not entirely unambiguous.

Cation exchange capacity, leachable cations and pore water chemistry

No significant changes in the CEC were observed for samples stored at temperatures up to 120ºC. A slight reduction seemed to occur after six months of heating. On longer heating, the CEC increased and even exceeded the value of the pristine material. However, these variations lay within the measurement error and were also influenced by the heterogeneity of the MX-80. However, the CEC of the MX-80 samples stored at $T = 150$ºC showed a distinct decrease in CEC of approximately 10% (Table 4, Fig. 7a).

No clear trends in the leachable Na^+, K^+, Mg^{2+} and Ca^{2+} concentrations with treatment time and temperature could be observed. The amount of leachable Na^+ of the bentonite MX-80 is, as expected, the highest in comparison with the other cations (57±4 cmol(+)/kg in pristine MX-80;
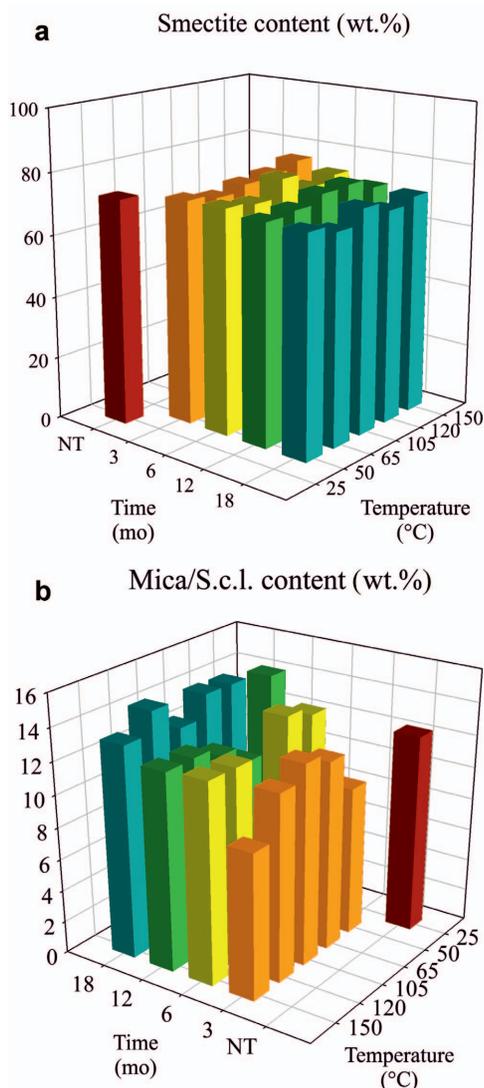
FIG. 4. Development of (a) the smectite content and (b) the sum of mica and mica-type layers/collapsed smectite layers (Mica/S.c.l.) in thermally treated MX-80 over time (NT...pristine MX-80).

TABLE 3. The changes of the smectite mean layer charge (MLC). All changes of the MLC after heating MX-80 over time are ambiguous when considering the measurement error (6-13%; Lagaly & Weiss, 1969).

MLC	Months				
(±0.02)	0	3	6	12	18
25ºC	0.28	–	–	–	–
50ºC	–	0.27	0.29	0.28	0.30
65ºC	–	0.27	0.29	0.28	0.29
105ºC	–	0.27	0.29	0.29	0.30
120ºC	–	0.27	0.28	0.28	0.29
150ºC	–	0.27	0.28	0.28	0.28
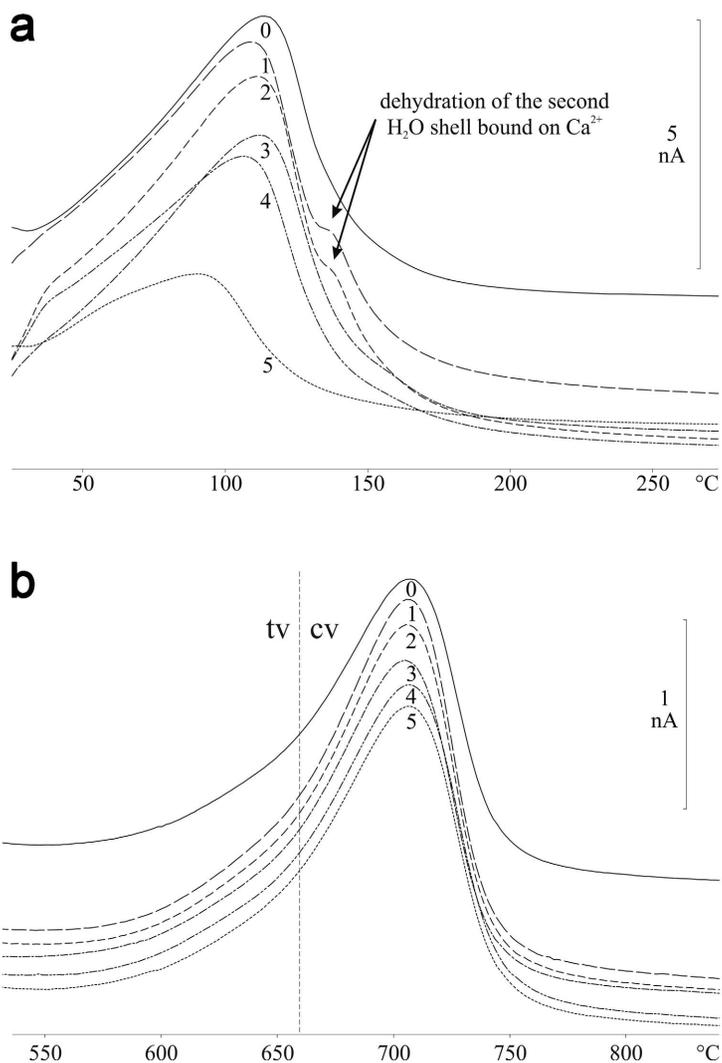
FIG. 5. Mass spectrometry curves of the thermally released H_2O from the pristine (curve 0) and MX-80 treated for 12 months at 50ºC (1), 65ºC (2), 105ºC (3), 120ºC (4), and 150ºC (5). A second dehydration shoulder evolved in the dehydration curves of the samples with higher saturation degree (1, 2) at a temperature of approximately 140ºC (a). The dehydroxylation curves (b) showed the predominant *cis*-vacant character of the octahedral layer in the dioctahedral smectite. The ratio of *trans*-vacant octahedral domains was low and stayed independent from the thermal treatment.

Table 4, Fig. 7b). However, considering the measurement error, a slight decrease could be observed for samples stored at 150ºC and at 120ºC for 18 months, which is similar to the trend in CEC.

Variation in the concentrations of leachable cations was influenced by the amount of added APW. In the samples with higher saturation degrees, the higher amount of added Mg^{2+} was mirrored in the higher amount of leachable Mg^{2+} (Table 4, Fig. 7c). The amount of leachable Ca^{2+}, instead, seemed to be more dependent on the dissolved Ca^{2+} from the soluble Ca-phases. The dissolution of calcite and gypsum/bassanite is a known effect that occurs during CEC determination when using complexes of Cu-triethylenetetramine

M. Valter and M. Plötze
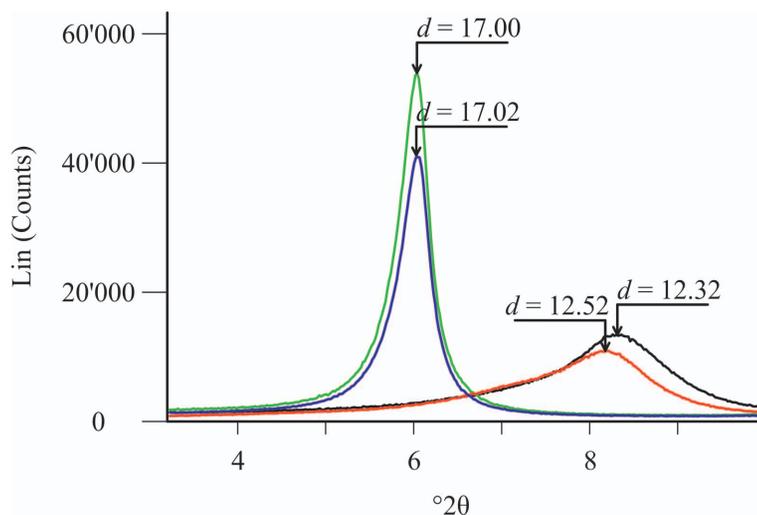
FIG. 6. Diffraction patterns showing the basal spacing of smectite in the pristine MX-80 (black) and heated at 150ºC for 18 months (red). The small increase was caused by partly exchange with bivalent cations. The basal spacing was similar after saturation with EG (green and blue curve respectively).

TABLE 4. Cation exchange capacity (CEC) (cmol(+)/kg), amount of leachable cations (ALC) and concentration of Na^+ in the pore water (PW) of the pristine and thermally treated MX-80. The concentration of leachable Ca^{2+} was overdetermined due to the dissolved water-soluble Ca-phases. The concentrations of Mg^{2+}, K^+ and Ca^{2+} in the PW are below the detection limit.

		CEC ±2	Na+ ±3	K+ ±1	Mg2+ ±1	Ca2+ ±3	Σ ±8	PW Na+ ± 0.3
MX-80 ESDRED "E"		84	57	1	6	36	100	1.8
	50ºC	84	56	2	7	39	104	7.3
	65ºC	86	56	2	8	38	104	5.3
3 months	105ºC	87	56	2	3	38	99	3.7
	120ºC	86	54	2	3	37	96	2.0
	150ºC	82	52	2	4	37	95	1.9
	50ºC	81	66	2	10	36	112	6.9
	65ºC	82	64	1	9	36	110	5.3
6 months	105ºC	82	61	2	4	38	105	4.1
	120ºC	80	60	1	3	36	100	1.7
	150ºC	77	53	2	4	38	97	1.6
	50ºC	83	61	2	10	38	111	6.5
	65ºC	84	58	1	8	36	103	5.4
12 months	105ºC	84	58	1	3	39	101	3.0
	120ºC	82	55	1	3	37	96	1.5
	150ºC	77	60	2	5	36	103	1.4
	50ºC	84	58	2	8	40	108	8.6
	65ºC	86	58	2	7	38	105	6.2
18 months	105ºC	87	57	2	2	42	103	3.3
	120ºC	84	52	2	3	38	95	1.8
	150ºC	79	51	2	4	38	95	2.1
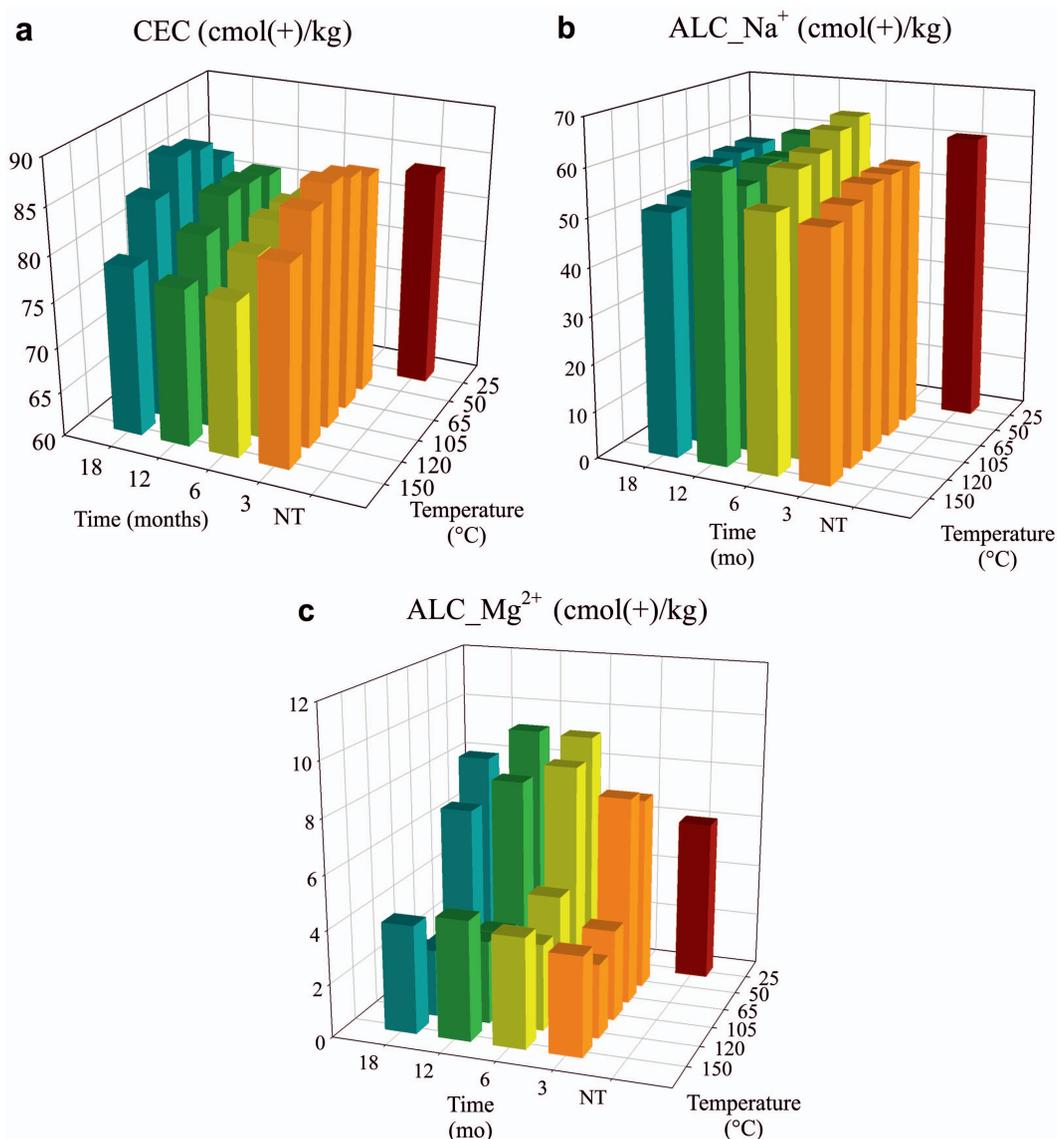
FIG. 7. Development of the CEC (a), the amount of leachable Na^+ (b) and Mg^{2+} (c) of the thermally treated MX-80 over time (NT...pristine MX-80). The decrease of the CEC and the amount of leachable Na^+ of samples heated up to 120ºC were within the error of the measurements (±2 and ±3 cmol(+)/kg respectively). The amount of the leachable Mg^{2+} depended on the added amount of the artificial pore water.

(Dohrmann & Kaufhold, 2010). The concentration of leachable Ca^{2+} of ~30 cmol(+)/kg is similar for all samples and originates from the dissolution of calcite and gypsum in the pristine material during the CEC analysis.

The major cation in the pore water of the MX-80 Na-bentonite was, as expected, Na^+. The content in the initial pore water of the pristine MX-80 was 1.8±0.3 cmol(+)/kg. The concentration of Na^+ in the pore water decreased from approximately 9 to 1 cmol(+)/kg. The values of K^+, Mg^{2+} and Ca^{2+} in the pore water of both heated and pristine bentonite, were below the limit of detection by AAS (Table 4; compare with Table 1).

Specific surface area

The specific surface area (SSA) of MX-80 decreased with increasing temperature over time (Table 5, Fig. 8a). The SSA of the pristine material (33 m^2/g) dropped by more than 50% to 15 m^2/g for the material stored at 150ºC for 18 months. The samples stored at other temperatures followed a similar trend. Even after remoulding, none of the samples reached the SSA values of the pristine material (Table 5, Fig. 8b). Only the SSA of samples stored at 120ºC for 12 and 18 months showed a clear trend of recovery reaching the values of samples heated for 3 and 6 months. Rather a tendency of a decreasing SSA was observed for samples stored at 50ºC.

Water vapour adsorption

The water vapour adsorption ability (WVAA) of the pristine MX-80 stored at 75% RH atmosphere was 17±0.3 wt.%. This value did not change up to 105ºC (Table 6, Fig. 9a). The WVAA decreased over time for MX-80 thermally treated at $T > 105$ºC to values of $13 - 12 \pm 0.3$ wt.%. The measurements of the remoulded samples showed a clear recovery of the WVAA reaching the value of the pristine material (Fig. 9b).

Water uptake under free swelling conditions

The WUC of the heated samples did not change up to 105ºC. Even taking into account that the variations of the WUC, values lay within the measurement error of about 25%, a tendency to decrease with time could be observed for samples heated at $T \geqslant 105$ºC for more than 12 months (Table 7, Fig. 10).

DISCUSSION

The analysis of the Na-bentonite MX-80 ESDRED "E" treated under near-field thermal and saturation conditions in a closed system showed an overall good stability of its mineral composition and physicochemical properties over the 18 month test period. Elevated temperatures ($\geqslant 105$ºC) causes some minor changes.

The smectite content seems to slightly decrease over time regardless of treatment temperature. However, this decrease is in the range of measurement error as well as additionally influ-

enced by the heterogeneity of the pristine MX-80 and is, therefore, rather ambiguous. Interestingly, the sum of mica and mica-type layers/collapsed smectite layers showed a weak opposite tendency (Fig. 4a, b). These changes could possibly indicate an initial illitization, which would be probably connected with the formation of interstratified illite/smectite (I/S). However, the insignificant increase of the coefficient of variation (CV) in the basal spacing from 0.2 of the pristine material to 0.38 of the sample with the highest content of mica and mica-type layers/collapsed smectite does not reflect a formation of interstratified I/S. The slight increase of the MLC from 0.28 to 0.30 for longer heated samples reflects more likely the formation of more highly charged smectite, rather than the formation of illite. In contrast, a very weak decrease of the MLC of smectite from initial 0.35 to 0.33±0.01 was found in the HEATER experiment (Plötze *et al.*, 2007). However, all these insignificant changes lie within the measurement error. Nevertheless, significant mineral changes in MX-80 were predicted by modelling its reaction with a representative geological fluid from Callovo-Oxfordian (COX) formation (Gaucher *et al.*, 2006) under repository thermal conditions ($T = 100$ºC) (Montes-H *et al.*, 2005; Marty *et al.*, 2010). Formation of saponite, vermiculite, illite, and chlorite by simultaneously decreasing content of smectite within 10,000 years was described.

The CEC is one of the most valuable properties for assessing the radionuclide retention of bentonite. Therefore, bentonite alteration connected with changes in CEC is an important process to monitor. A weak increase of the CEC towards the heating source was observed in the *in-situ* ABM and LOT experiments (Nagra, 2011; Svensson *et al.*, 2011, Olsson & Karnland, 2011). The investigation of long-term heated samples in an open system showed, after an initial decrease of the CEC within one year, a slight increase on further heating at temperatures >120ºC (Valter & Plötze, 2010). The tendency for CEC increase over time after an initial decrease was also observed in the present work. However, the measured CEC variations are close to the analytical error of the method in all these experiments. In contrast, in the present work, the CEC of the samples stored above the critical temperature of 120ºC decreases non-ambiguously. The same observation was reported by Gómez-Espina & Villar (2010). This decrease in CEC cannot be explained with the measured

TABLE 5. The specific surface area (SSA) of thermally treated MX-80 before and after remoulding determined by N$_2$-BET.

		SSA (m^2/g) ±2%			SSA (m^2/g) ±2%
MX-80 ESDRED "E"		33.1			
	50ºC	28.9		50ºC	23.6
	65ºC	26.7		65ºC	23.3
3 months	105ºC	24.0	12 months	105ºC	20.8
	120ºC	22.8		120ºC	14.9
	150ºC	16.8		150ºC	14.5
	50ºC	30.6		50ºC	25.9
	65ºC	29.0		65ºC	24.8
6 months	105ºC	22.1	18 months	105ºC	20.4
	120ºC	23.9		120ºC	15.0
	150ºC	17.7		150ºC	14.8
Remoulded material					
3 months	50ºC	24.8	12 months	50ºC	19.8
	120ºC	23.9		120ºC	23.2
6 months	50ºC	16.3	18 months	50ºC	29.3
	120ºC	21.3		120ºC	25.2

changes in MLC. The lower CEC is most probably caused by a stronger fixation of the exchangeable cations and the higher content of mica-type layers/ collapsed smectite.

Olsson & Karnland (2011) reported in the LOT project a redistribution of Ca-sulfate phases. Their results indicate the dissolution of gypsum in the colder part of the bentonite barrier at the contact to
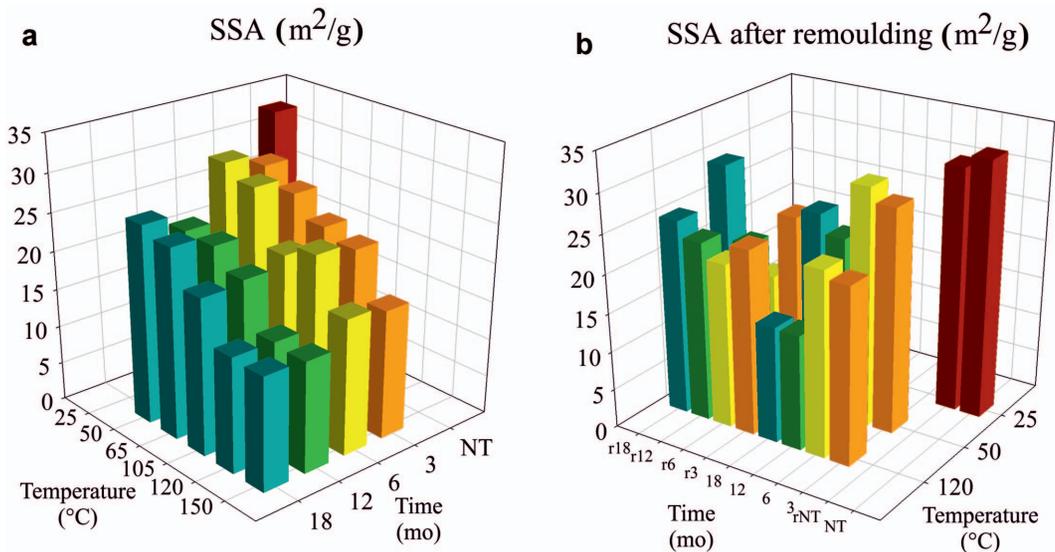
FIG. 8. Development of the specific surface area (SSA) of thermally treated MX-80 over time (a) and (b) after remoulding of selected samples (r...remoulded samples, NT...pristine MX-80).

TABLE 6. The water vapour adsorption ability at 75% relative humidity (WVAA) of thermally treated MX-80 before and after remoulding.

		WVAA (wt.%)			WVAA (wt.%)
MX-80 ESDRED "E"		16.9			
	50ºC	16.7		50ºC	16.5
	65ºC	16.5		65ºC	16.5
3 months	105ºC	16.1	12 months	105ºC	15.9
	120ºC	13.4		120ºC	12.4
	150ºC	12.6		150ºC	12.0
	50ºC	16.6		50ºC	16.8
	65ºC	16.5		65ºC	16.8
6 months	105ºC	16.2	18 months	105ºC	16.3
	120ºC	13.2		120ºC	12.8
	150ºC	12.3		150ºC	12.2
Remoulded material					
	50ºC	16.8		50ºC	16.9
3 months	120ºC	15.8	12 months	120ºC	15.5
	50ºC	16.8			
6 months	120ºC	15.5			

the host rock with ground water and the precipitation of anhydrite in the bentonite close to the heater within almost six years. These observations could be reproduced also by modelling (Itälä & Olin, 2011). In the closed systems of our experiment, such redistribution was excluded. Gypsum was dissolved in the samples with higher saturation degrees $S_r > 0.5$ at temperatures $T < 105$ºC. The Ca^{2+} and Mg^{2+} from the dissolved gypsum and from the added APW exchanged the Na^+ in the
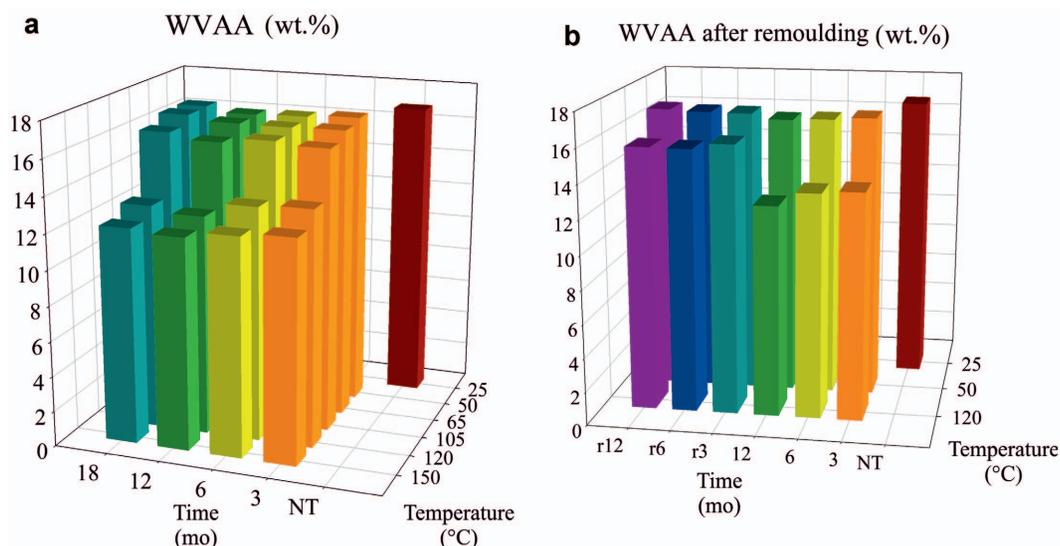
FIG. 9. Development of the water vapour adsorption ability at 75% relative humidity (WVAA) of thermally treated MX-80 over time (a) and (b) after remoulding of selected samples (r...remoulded samples, NT...pristine MX-80).

TABLE 7. The water uptake of thermally treated MX-80 under free swelling conditions.

		Water uptake after 24 h (wt.%)
MX-80 ESDRED "E"		613%
	50ºC	781%
	65ºC	725%
3 months	105ºC	781%
	120ºC	650%
	150ºC	613%
	50ºC	688%
	65ºC	775%
6 months	105ºC	638%
	120ºC	706%
	150ºC	631%
	50ºC	688%
	65ºC	662%
12 months	105ºC	709%
	120ºC	627%
	150ºC	566%
	50ºC	606%
	65ºC	606%
18 months	105ºC	488%
	120ºC	463%
	150ºC	463%

FIG. 10. Development of the water-uptake capacity (WUC) of thermally treated MX-80 over time (NT...pristine MX-80).

smectite interlayer. This is clearly visible in the dehydration curves of the bentonites in thermal analysis. The dehydration curves show a shoulder at approximately 140ºC, which corresponds to the release of the second water layer attached to the bivalent cations (Emmerich, 2011). In the samples stored at temperatures > 65ºC gypsum dehydrated to bassanite but not to anhydrite. For this thermal decomposition probably higher temperatures or longer time are necessary.

The type of adsorbed and exchangeable cations influences such mechanical and physicochemical properties like plasticity and shear strength, water adsorption and swelling, specific surface area, microstructure and hydraulic conductivity. The amount of leachable Na^+ of the bentonite MX-80 is, as expected, the highest in comparison with the other cations (Table 4, Fig. 7b). The amount of leachable cations was influenced by the added amount of APW. The Na^+ in the bentonite was exchanged by the K^+, Mg^{2+} and Ca^{2+} particularly in the samples with higher saturation degree ($S_r = 1-0.75$). Additionally, the Na^+ was partly exchanged by Ca^{2+} from dissolved gypsum and calcite. Consequently, the concentration of Na^+ in the pore water in these samples is higher as the initial concentration (7−9 *vs.* 2 cmol(+)/kg, Tab. 4). The same cation exchange was observed in the LOT experiment (Olsson & Karnland, 2011; Itälä & Olin, 2011).

Generally, the specific surface area of Ca/Mg-bentonites is higher than that of Na-bentonites (Kaufhold *et al.*, 2010b). This is in agreement with our findings. The samples with the higher Ca^{2+}/Mg^{2+} content showed higher values of SSA. The SSA decreased by about 50% after thermal treatment with increasing temperature over time. A similar decrease of SSA was also observed in the ABM- project and the HEATER experiment (Nagra, 2011; Plötze, *et al.*, 2007). The variations in SSA between the Ca/Mg- and Na-bentonite were explained with differences in their microporosity from the quasi-crystalline overlap region of smectite and the accessible area of the interlayer (Kaufhold *et al.*, 2010b), i.e. the "roughness" of the smectite platelet edges. However, with increasing treatment temperature, the SSA decreases also for samples with higher amount of leachable Na^+. Therefore, additional effects on the microporosity have to be considered, e.g. dissolution and precipitation processes leading to aggregation effects. The influence of such effects was
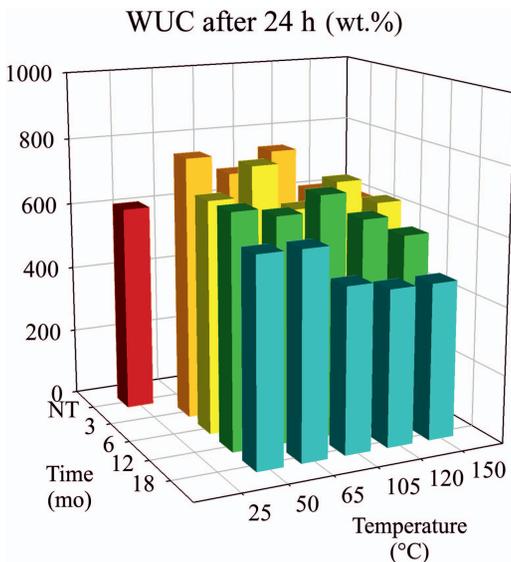
investigated by measurement of the SSA of some samples after remoulding. However, the changes in SSA after remoulding bordered the line of analytical error and did not show non-ambiguous trends (Table 5, Fig. 8b). None of the samples reached the SSA value of the pristine material. Only for samples stored at 120ºC for 12 and 18 months, a tendency of SSA recovery was observed reaching the values of samples heated over shorter time.

Swelling is a typical feature of bentonite when in contact with water in gaseous or liquid form. The amount of adsorbed water depends on the type of smectite, the layer charge density, and on the type of exchangeable cations in the interlayer (Laird, 1999; Kaufhold *et al.*, 2010a). In addition, the water adsorption under free swelling conditions (WUC) is strongly affected by the microporosity of bentonite (Kaufhold *et al.*, 2010a). The lower the amount of leachable Na^+, the lower is the WUC (Kaufhold *et al.*, 2010a). The WUC of the thermally treated MX-80 in the presented experiment decreased with increasing temperature over time and had a similar development as the SSA. This decrease could be observed especially for samples heated at $T \geqslant 105$ºC for more than 12 months (Table 7, Fig. 10). However, these samples have a higher content of leachable Na^+ and consequently should have a higher WUC. The sole influence of the type of the interlayer cation could be thus excluded. The WUC of the thermally treated bentonite is, as the SSA, rather dependent on the bentonite aggregation and microstructure.

A link between the SSA and the WVAA has been observed previously by Kaufhold *et al*. (2010b). Both methods are based on gas adsorption. However, the adsorption mechanisms are rather different. In contrast to N_2, which will be adsorbed on external surfaces and micropores, the polar water molecules mainly hydrate the adsorbed cations. The WVAA is therefore strongly influenced by the type of these cations. However, at the applied relative humidity of 75% the difference in the water adsorption between Ca^{2+} and Na^+ is not significant (Bérend *et al.*, 1995; Cases *et al.*, 1997; Plötze & Kahr, 2003). The presented results show in WVAA two plateaus independent from time with a significant drop at $T > 105$ºC (Fig. 9). A similar decrease of the WVAA of MX-80 (by approximately 20%) after its long-term heating in an open system at temperatures up to 200ºC was also described by Valter & Plötze (2010). The clear

recovery of the WVAA reaching the value of the pristine material was observed for remoulded samples (Fig. 9b). This behaviour can be explained by cementing processes during thermal treatment, which "glue" the smectite platelets. The remoulding procedure breaks up the cemented platelets. The water molecules can enter the interlayer and hydrate the interlayer cations. The WVAA of the thermally treated bentonite is rather dependent on the bentonite aggregation and microstructure than caused by the so-called Couture effect, which describes an irreversibly reduced water uptake of bentonite after steam treatment at 250ºC (Couture, 1985).

CONCLUSIONS

The analysis of the Na-bentonite MX-80 treated under near-field thermal and saturation conditions in a closed system showed a high mineralogical stability over the 18-months test period. Only minor changes occurred at elevated temperature ($\geqslant 105$ºC): (i) The smectite content seems to decrease slightly over time regardless of treatment temperature. However, this decrease is in the range of measurement error as well as being additionally influenced by the heterogeneity of the pristine MX-80. Furthermore, the insignificant increase of the coefficient of variation in the basal spacing and of the MLC indicated more likely the formation of higher charged smectite, rather than of illite. Amorphous silica could also not be detected. (ii) The gypsum content did not change in samples stored at temperatures below 105ºC. At $T \geqslant 105$ºC gypsum dehydrated to bassanite. (iii) The calcite content showed a subtle tendency of decrease with temperature.

Whereas the mineralogical alterations are close to insignificant, considerable changes in physicochemical properties were observed: (i) The cation exchange capacity is one of the most valuable properties for assessing the radionuclide retention of bentonite. A very weak increase towards the heating source was observed in several in-situ experiments. In contrast, in our experiment, the CEC decreased non-ambiguously for the samples stored above the critical temperature of 120ºC. (ii) A slight conversion from the sodium to an earth alkali form of the bentonite was observed. The Ca^{2+} and Mg^{2+} from the dissolved Ca-phases (gypsum, calcite) and from the added artificial pore water exchanged the Na^+ in the smectite interlayer. The

type of exchangeable cations as well as aggregation processes connected with dissolution/precipitation influenced physicochemical properties like water adsorption and swelling, specific surface area and microstructure. (iii) The SSA decreased by ~50% after thermal treatment with increasing temperature over time. (iv) The water uptake capacity under free swelling conditions decreased with increasing temperature over time especially for samples heated at $T \geqslant 105$ºC for more than 12 months. (v) The water vapour adsorption ability showed a significant drop at $T = 120$ºC. The ability to recover by mechanical remoulding can be explained with cementing processes during the thermal treatment.

The observed alterations are mostly subtle. However, temperatures $\geqslant 120$ºC had a remarkable negative influence on different properties of MX-80.

REFERENCES

Bérend I., Cases J.M., François M., Uriot J.P., Michot L., Masion A. & Thomas F. (1995) Mechanism of adsorption and desorption of water vapor by homoionic montmorillonites: 2. The Li$^+$, Na$^+$, K$^+$, Rb$^+$ and Cs$^+$-exchanged forms. *Clays and Clay Minerals*, **43**, 324–336.

Bergmann J. & Kleeberg R. (1998) Rietveld analysis of disordered layer silicates. *Materials Science Forum*, **278–281**, 300–305.

Brindley G.W. & Brown G. (1980) X-ray diffraction procedures for clay mineral identification. Pp. 305–359 in: *Crystal Structures of Clays Minerals and their X-ray Identification* (G.W. Brindley & G. Brown, editors). Monograph **5**, Mineralogical Society, London.

Brunauer S., Emmet P.S. & Teller E. (1938) Adsorption of gases in multimolecular layers. *Journal of American Chemical Society*, **60**, 309–319.

Cases J.M., Bérend I., François M., Uriot J.P., Michot L.J. & Thomas F. (1997) Mechanism of adsorption and desorption of water vapor by homoionic montmorillonite: 3. The Mg^{2+}, Ca^{2+}, Sr^{2+} and Ba^{2+} exchanged forms. *Clays and Clay Minerals*, **45**, 8–22.

Chamley H. (1989) *Clay Sedimentology*, 411–414. Springer-Verlag, Berlin.

Couture R.A. (1985) Steam rapidly reduces the swelling capacity of bentonite. *Letters to Nature*, **318**, 50–52.

DIN 18132 (1995) *Determination of Water Absorption*. DIN Deutsches Institut für Normung, Berlin.

DIN ISO 11465 (1996) *Determination of Dry Matter and Water Content on a Mass Basis*. DIN Deutsches Institut für Normung, Berlin.

Dohrmann R. & Kaufhold S. (2010) Determination of exchangeable calcium of calcareous and gypsiferous bentonites. *Clays and Clay Minerals*, **58**, 79–88.

Emmerich K. (2011) Thermal analysis in the characterization and processing of industrial minerals. Pp. 129–170 in: *Advances in the Characterization of Industrial Minerals* (G.E. Christidis, editor). European Mineralogical Union and the Mineralogical Society of Great Britain & Ireland, London.

enresa (2000) *FEBEX project, Full-scale engineered barriers experiment for a deep geological repository for high level radioactive waste in crystalline host rock*. Final report. enresa, Madrid.

Galán E. (2006) Genesis of clay minerals. Pp. 1129–1162 in: *Handbook of Clay Science* (F. Bergaya, B. Theng & G. Lagaly, editors). Elsevier, Amsterdam.

Gaucher É.C., Blanc P., Bardot F., Braibant G., Buschaert S., Crouzet C., Gautier A., Girard J.P., Jacquot E., Lassin A., Negrel G., Tournassat C., Vinsot A. & Altmann S. (2006) Modelling the porewater chemistry of the Callovian–Oxfordian formation at a regional scale. *Comptes Rendus Geoscience*, **338**, 917–930.

Göbel I., Alheid H.J., Jockwer N., Mayor J.C., García-Siñeriz J.L., Alonso E., Weber H., Plötze M., Klubertanz G. & Rothpletz C.A. (2006) *Heater Experiment: Rock and bentonite Thermo-Hydro-Mechanical (THM) processes in the near-field of a thermal source for development of deep underground high level radioactive waste repositories*. Euratom.

Gómez-Espina R. & Villar M.V. (2010) Geochemical and mineralogical changes in compacted MX-80 bentonite submitted to heat and water gradients. *Applied Clay Science*, **47**, 400–408.

Herbert H.J., Kasbohm J., Sprenger H., Frenández A.M. & Reichelt C. (2008) Swelling pressures of MX-80 bentonite in solutions of different ionic strength.

Physics and Chemistry of the Earth, **33**, S327–S342.

Itälä A. & Olin M. (2011) Chemical evolution of bentonite buffer in a final repository of spent nuclear fuel during the thermal phase. *Nuclear Technology*, **174**, 342–352.

Kahr G. & Müller Vonmoos M. (1982) *Wärmeleitfähigkeit von Bentonit MX80* und *von Montigel nach der Heizdrahtmethode*. Nagra Technical Report NTB 82-06. Nagra, Baden.

Kasbohm J., Pusch R., Nguyen-Thanh L. & Hoang-Ming T. (2012) Lab-scale performance of selected expandable clays under HLW repository conditions. *Environmental Earth Sciences*. DOI 10.1007/s12665-012-2085-1

Kaufhold S. & Dohrmann R. (2009) Stability of bentonites in salt solutions I. Sodium chloride. *Applied Clay Science*, **45**, 171–177.

Kaufhold S. & Dohrmann R. (2010) Stability of bentonites in salt solutions II. Potassium chloride solution – Initial step of illitization? *Applied Clay Science*, **49**, 98–107.

Kaufhold S. & Dohrmann R. (2011) Stability of bentonites in salt solutions III. Calcium hydroxide. *Applied Clay Science*, **51**, 300–307.

Kaufhold S., Dohrmann R. & Klinkenberg M. (2010a) Water uptake capacity of bentonites. *Clays and Clay Minerals*, **58**, 37–43.

Kaufhold S., Dohrmann R., Klinkenberg M., Siegesmund S. & Ufer K. (2010b) N2-BET specific surface area of bentonites. *Journal of Colloid and Interface Science*, **349**, 275–282.

Keeling P.S., Kirby E.C. & Robertson R.H. (1980) Moisture adsorption and specific surface area. *Transactions and Journal of the British Ceramic Society*, **79**, 36–40.

Lagaly G. (1994) Layer charge determination by alkylammonium ions. Pp. 1–46 in: *Layer Charge Characteristics of 2:1 Silicate Clay Minerals* (A.R. Mermut, editor). The Clay Minerals Society, Boulder, Colorado, USA.

Lagaly G. & Weiss A. (1969) Determination of the layer charge in mica-type layer silicates. Pp. 61–80 in: *Proceedings of the International Clay Conference, Vol. 1* (L. Heller, editor). Israel Universities Press, Tokyo.

Laine H. & Karttunen P. (2010) *Long-Term Stability of Bentonite*, Working Report 2010-53. Posiva Oy, Eurajoki.

Laird D.A. (1999) Layer charge influences on the hydration of expandable 2:1 phyllosilicates. *Clays and Clay Minerals*, **47**, 630–636.

MacEwan D.M.C. & Wilson M.J. (1980) Interlayer and intercalation complexes of clay minerals. Pp. 197–248 in: *Crystal Structures of Clay Minerals and their X-ray identification* (G.W. Brindley & G. Brown, editors). Mineralogical Society, London.

Madejová J., Balan E. & Petit S. (2011) Application of vibrational spectroscopy to the characterization of phyllosilicates and other industrial minerals. Pp. 171–226 in: *Advances in the Characterization of Industrial Minerals* (G.E. Christidis, editor). European Mineralogical Union and the Mineralogical Society of Great Britain & Ireland, London.

Mäder U.K. (2009) *Reference pore water for the Opalinus clay and "Brown Dogger" for the provisional safety-analysis in the framework of the sectorial plan – interim results (SGT-ZE)*. Nagra Work Report NAB 09-14. Nagra, Wettingen.

Madsen F.T. & Kahr G. (1992) Wasserdampfadsorption und spezifische Oberfläche von Tonen. Pp. 165–179 in: *Contributions to Annual Meeting Hannover* (H. Graf v. Reichenbach). DTTG, Hannover, Germany.

Marty N.C.M., Fritz B., Clément A. & Michau N. (2010) Modelling the long term alteration of the engineered bentonite barrier in an underground radioactive waste repository. *Applied Clay Science*, **47**, 82–90.

Meier L.P. & Kahr G. (1999) Determination of the cation exchange capacity (CEC) of clay minerals using the complexes of Copper (II) ion with Triethylenetetramine and Tetraethylenepentamine. *Clays and Clay Minerals*, **47**, 386–388.

Montes-H G. & Geraud Y. (2004) Sorption kinetic of water vapour of MX80 bentonite submitted to different physical–chemical and mechanical conditions. *Colloids and Surfaces A: Physicochemical and Engineering Aspects*, **235**, 17–23.

Montes-H G., Fritz B., Clement A. & Michau N. (2005) Modelling of geochemical reactions and experimental cation exchange in MX80 bentonite. *Journal of environmental management*, **77**, 35–46.

Moore D.M. & Reynolds R.C. (1997) *X-Ray Diffraction and the Identification and Analysis of Clay Minerals*, 2nd edition. Oxford University Press, Oxford.

Nagra (2002) *Project Opalinus Clay – Demonstration of disposal feasibility for spent fuel, vitrified high-level waste and long-lived intermediate-level waste (proof of waste disposal)*. Nagra Technical Report NTB 02-05. Nagra, Wettingen.

Nagra (2011) *Alternative Buffer Material, Status Report*. Nagra Technical Report NAB 11-19. Nagra, Wettingen.

Olsson S. & Karnland O. (2011) Mineralogical and chemical characteristics of the bentonite in the A2 test parcel of the LOT field experiments at Äspö HRL, Sweden. *Physics and Chemistry of the Earth*, **36**, 1545–1553.

Perdrial J.N. & Warr L.N. (2011) Hydration behavior of MX80 bentonite in a confined-volume system: Implications for backfill design. *Clays and Clay Minerals*, **59**, 640–653.

Plötze M. & Kahr G. (2003) Swelling pressure and suction of clays. Pp. 479–483 in: *Geotechnics of Soft*

Soils (P.A. Vermeer, H.F. Schweiger, M. Karstunen & M. Cudny, editors). VGE, Essen.

Plötze M. & Weber H.P. (2007) *ESDRED: Emplacement tests with granular bentonite MX-80. Laboratory results from ETH Zürich.* Nagra Work Report NAB 07-24. Nagra, Wettingen.

Plötze M., Kahr G., Dohrmann R. & Weber H. (2007) Hydro-mechanical, geochemical and mineralogical characteristics of the bentonite buffer in a heater experiment: The HE-B project at the Mont Terri Rock Laboratory. *Physics and Chemistry of the Earth*, **32**, 730−740.

Olis A.C., Malla, P.B. & Douglas L.A. (1990) The rapid estimation of the layer charges of 2:1 expanding clays from a single alkylammonium ion expansion. *Clay Minerals*, **25**, 39−50.

Pusch R. (2000) *On the effect of hot water vapor on MX-80 clay.* SKB Technical Report TR-00-16. SKB, Stockholm.

Pusch R. (2001) *The buffer and backfill handbook, Part 2: Materials and techniques*. SKB Technical Report TR-02-12. SKB, Stockholm.

Pusch R. (2006) Clays and nuclear waste management. Pp. 703−716 in: *Handbook of Clay Science* (F. Bergaya, B.K.G. Theng & G. Lagaly, editors). Elsevier, Amsterdam.

Russell S. & Facella J.A. (2006) Progress towards long-term management of used nuclear fuel in Canada. Pp. 39−54 in: *Geological Challenges in Radioactive Waste Isolation, Fourth Worldwide Review* (P.A. Witherspoon & G.S. Bodvarsson, editors).

University of California, Berkeley, California, USA.

Sato R., Sasaki T., Ando K., Smith P.A. & Schneider J.W. (1998) *Calculations of the temperature evolution of a repository for spent fuel in crystalline and sedimentary rocks.* Nagra Technical Report NTR 97-02. Nagra, Wettingen, Switzerland.

Senger R. & Ewing J.J. (2008) *Evolution of temperature and water content in bentonite buffer: Detailed modelling of two phase flow processes associated with the early closure period.* Nagra Work Report NAB 08-32. Nagra, Wettingen.

Svensson D., Dueck A., Nilsson U., Olsson S., Sandén T., Lydmark S., Jägerwall S., Pedersen K. & Hansen S. (2011) *Alternative buffer material − Status of the ongoing laboratory investigation of reference materials and test package 1.* SKB Technical Report TR-11-06. SKB, Stockholm.

Valter M. & Plötze M. (2010) New observations in behaviour of clays after their long-term thermal treatment. Pp. 515 in: *Clays in Natural & Engineered Barriers for Radioactive Waste Confinement, Abstracts*. Andra, Nantes.

Villar M.V. & Lloret A. (2007) Dismantling of the first section of the FEBEX in situ test: THM laboratory tests on the bentonite blocks retrieved. *Physics and Chemistry of the Earth*, **32**, 716−729.

Zhang G., Germaine J.T., Torrence Martin R. & Whittle A.J. (2003) A simple sample-mounting method for random powder X-ray diffraction. *Clays and Clay Minerals*, **51**, 218−225.